AFRL-SR-AR-TR-09-0258

REPORT DOCUMENTATION PAGE

PLEASE DO NOT RETURN YOUR FORM TO THE ABOVE ORGANIZATION.

1. REPORT DATE *(DD-MM-YYYY)*	2. REPORT TYPE	3. DATES COVERED *(From - To)*
	Final	

4. TITLE AND SUBTITLE
THE USE OF MODELING BASED, PHYSICAL SIMULATION TO REVEAL THE RELATIONSHIP BETWEEN PROCESS PARAMETERS AND MICROSTRUCTURAL EVOLUTION IN THERMAL STIR PROCESSED (TSP) TI6A1-4V

5a. CONTRACT NUMBER
FA9550-07-1-0282

5b. GRANT NUMBER

5c. PROGRAM ELEMENT NUMBER

6. AUTHOR(S)
Schneider, Judy

5d. PROJECT NUMBER

5e. TASK NUMBER

5f. WORK UNIT NUMBER

7. PERFORMING ORGANIZATION NAME(S) AND ADDRESS(ES)
Department of Mechanical Engineering
Mississippi State University
Box 9552
Mississippi State, MS 39762

8. PERFORMING ORGANIZATION REPORT NUMBER

9. SPONSORING/MONITORING AGENCY NAME(S) AND ADDRESS(ES)
Joan Fuller
AFOSR
875 N Randolph Street
Arlington, VA

10. SPONSOR/MONITOR'S ACRONYM(S)

11. SPONSOR/MONITOR'S REPORT NUMBER(S)

12. DISTRIBUTION/AVAILABILITY STATEMENT

13. SUPPLEMENTARY NOTES

14. ABSTRACT

The initial work statement targeted quantifying the hot working conditions experienced by titanium during friction stir welding/processing (FSW/P). Of particular interest was the identification of the hot working conditions (i.e. strain rate, strain, and temperature) required to refine the grains in the weld zone or nugget. Using a kinematic approach toward modeling of the FSW/P, the instantaneous shear strain rate encountered by the material entering the rotation plug around the weld tool is estimated to be in the range of 103 to 106 s-1 at strains levels in excess of 50. A similar level of grain refinement has been reported in metal chips formed during cutting operations where the shear strain rate is estimated to be in the range of 103 to 106 s-1, but at strain levels less than 5. Both these processes are predicted to instantaneously impart strain rates on the order of ballistic impact on the metal. In contrast grain refinement has also been reported in equal channel angular extrusion (ECAE) where the grain size reduction has been correlated with the increasing amount of strain achieved by multi passes at quasi-static strain rates. The motivation for this study is furthering our understanding of the mechanics responsible for grain refinement as influenced by ballistic level sheer strain rate and/or shear strain

15. SUBJECT TERMS
shear, strain, refinement, titanium, welding, angular, extrusion, quasi, static

16. SECURITY CLASSIFICATION OF:			17. LIMITATION OF ABSTRACT	18. NUMBER OF PAGES	19a. NAME OF RESPONSIBLE PERSON
a. REPORT	b. ABSTRACT	c. THIS PAGE			Joan Fuller
					19b. TELEPHONE NUMBER *(Include area code)* 703-696-7236

Final Report

Grant/Contract Title: THE USE OF MODELING BASED, PHYSICAL SIMULATION TO REVEAL THE RELATIONSHIP BETWEEN PROCESS PARAMETERS AND MICROSTRUCTURAL EVOLUTION IN THERMAL STIR PROCESSED (TSP) TI6A1-4V

Grant/Contract Number: FA9550-07-1-0282

Judy Schneider, Associate Professor
Department of Mechanical Engineering
Mississippi State University

I. Project Summary

The initial work statement targeted quantifying the hot working conditions experienced by titanium during friction stir welding/processing (FSW/P). Of particular interest was the identification of the hot working conditions (i.e. strain rate, strain, and temperature) required to refine the grains in the weld zone or nugget. Using a kinematic approach toward modeling of the FSW/P, the instantaneous shear strain rate encountered by the material entering the rotation plug around the weld tool is estimated to be in the range of 10^3 to 10^6 s^{-1} at strains levels in excess of 50. A similar level of grain refinement has been reported in metal chips formed during cutting operations where the shear strain rate is estimated to be in the range of 10^3 to 10^6 s^{-1}, but at strain levels less than 5. Both these processes are predicted to instantaneously impart strain rates on the order of ballistic impact on the metal. In contrast grain refinement has also been reported in equal channel angular extrusion (ECAE) where the grain size reduction has been correlated with the increasing amount of strain achieved by multi passes at quasi-static strain rates. The motivation for this study is furthering our understanding of the mechanics responsible for grain refinement as influenced by ballistic level shear strain rate and/or shear strain.

The hot working or processing behavior of titanium alloys is being established based on correlating the phase thermodynamics and the metal forming conditions defined by a combination of physical simulation and theoretical modeling of the friction stir process. **The focus of our project is not process development per se, but rather understanding how the microstructures were generated using physical simulation guided by input from kinematic modeling studies [1].**

II. Background

High temperature materials, including Titanium and its alloys have widespread interest among the NASA, Air Force, and Navy. The workhorse alloy, Ti-6Al-4V, is used in both cast and wrought forms. While the cast and hot isostatically pressed (HIPed) lamellar microstructure is relatively resistant to fatigue crack growth, the α/β processed microstructure with equiaxed α provides increased resistance to fatigue crack initiation [2]. Thermomechanical processing of the two phase Ti alloy either above or below the βtransus results in differing microstructures [3]. This allows inference of the temperature by examination of the resulting microstructure. In the

metal working processes being investigated, adiabatic heating also contributes to the heat input and must be quantified.

Mechanisms responsible for grain refinement at conditions of ballistic impact are unknown [4]. This maybe due in part to the short time frame in which the impact and resulting microstructural refinement occurs. The temperatures during impact are also not known with estimates of adiabatic heating based on a 90% conversion efficiency, independent of the strain rate [5].

III. Modeling

The processing history or hot working parameters that result in recrystallization of FSW/P weld nugget and chips formed during metal cutting are unknown. In studies of FSW/P of Ti alloys, the reported temperature range is reported to be in the range of 950-1467°C [2, 3, 6-8]. The β transus temperature for Ti is reported in the range of 950-980° C at quasi static conditions [2, 3]. Although there is interest in limiting the FSW/P temperature to avoid the non-homogeneous microstructural changes which would accompany the localized α to β phase transformation, there has been no reported success in the open literature [8]. This may suggest that the adiabatic heating associated with the high shear strain rate of the process is higher than estimated using a 90% energy conversion to heat.

Through marker studies conducted at the NASA-MSFC [9-15], the presence of a severe shear zone has been defined that encompasses a rotating plug of metal as illustrated in Figure 1. Figure 2 shows the metal within this rotating metal plug is significantly refined. This report documents studies undertaken to determine if the conditions imposed on the metal entering the shear zone are severe enough to drive an instantaneous recrystallization phenomenon rather than the more traditionally understood recrystallization process. Adiabatic shear temperatures are estimated on the basis of a conversion of energy to heat. This is assumed to be a constant, independent of the shear strain rate.

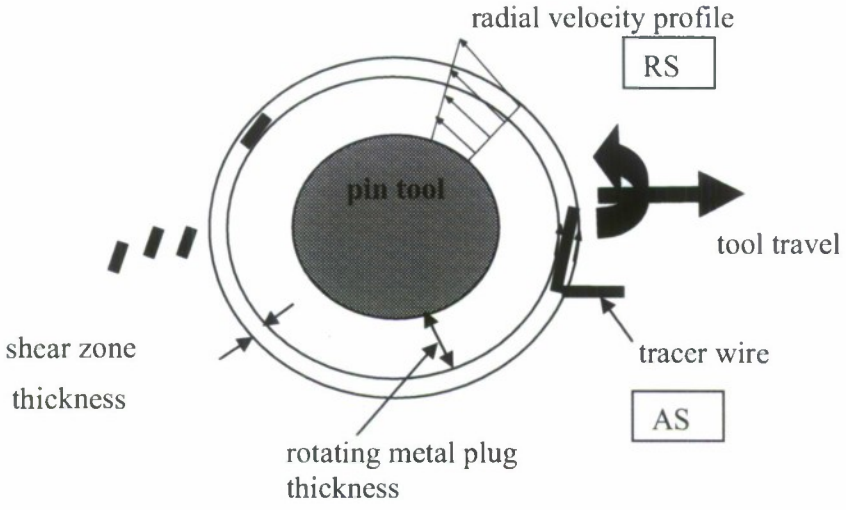

Figure 1. Plan (top view) of metal in vicinity of weld tool. Tungsten wires (0.001") were used to trace out location of shear zone a finite distance from the tool surface.

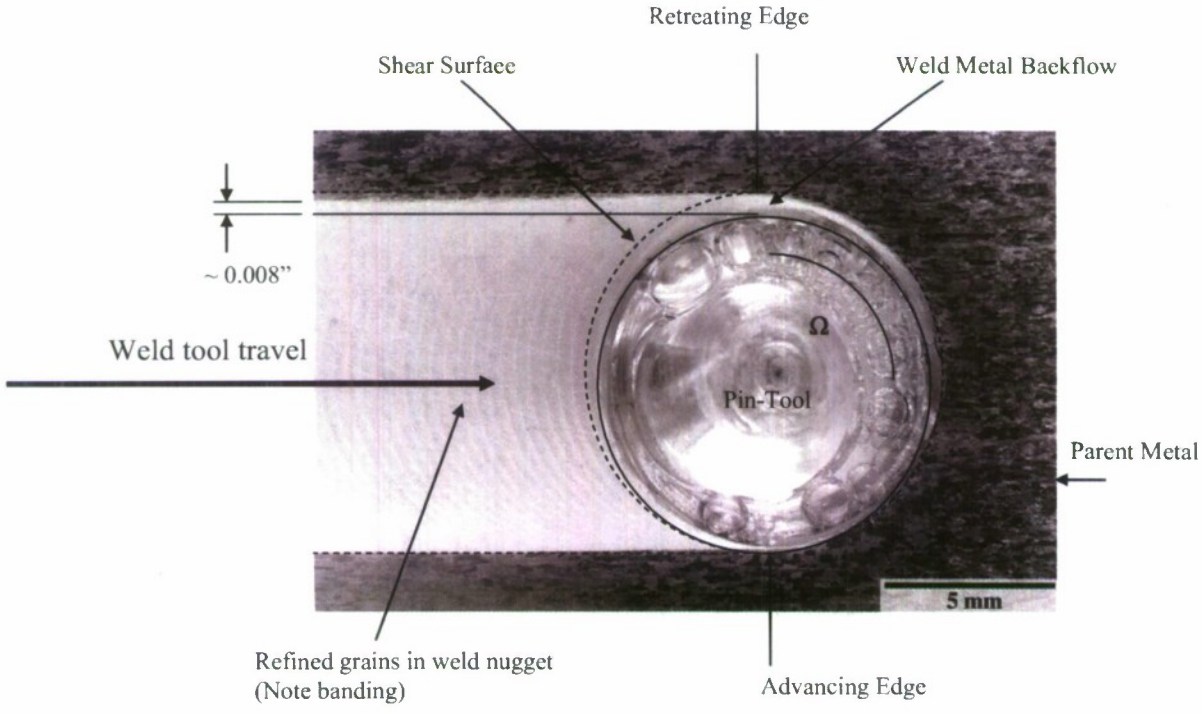

Figure 2. Plan (top) view of FSW with pin tool removed. Specimen has been metallographically sectioned to mid-panel thickness. The material surrounding the pin tool is refined in comparison with the parent material.

A) Kinematic Modeling

Table I summarizes the imposed metal working conditions during FSW/P, estimated using the Nunes Kinematic model [1]. The linear strain increment imposed on the joint seam is based on the relationship given in equation 1, where R=pin tool radius, Ω=tool angular velocity, and V=weld travel speed.

$$\Delta\gamma \approx \frac{R\Omega}{V\cos\theta} \geq \frac{R\Omega}{V} \qquad \text{(eqn. 1)}$$

Equation 2 approximates the shear strain rate, where δ = shear zone thickness. Based on these relationships, the pin tool rotation controls the amount of strain and strain rate while the strain is inversely proportional to the weld travel velocity. The shear zone thickness is estimated at 0.02 cm under further validation and verification can be made.

$$\dot{\gamma} = \frac{\Delta\gamma}{\Delta t} \approx \frac{\left(\frac{R\Omega}{V\cos\theta}\right)}{\left(\frac{\delta}{V\cos\theta}\right)} = \frac{R\Omega}{\delta} \qquad \text{(eqn. 2)}$$

Table I. Predicted Metal working conditions during FSWing.

Condition	Value
shear strain	> 50
shear strain rate	10^3 to 10^8 s^{-1}
est. temperature	0.6 to 0.9 Tmp

Based on the relationships given in equations 1 and 2, the strain rate of the process is relatively insensitive to the typical range of processing conditions utilized in FSW. To achieve an order of magnitude change in the strain rate would require an order of magnitude decrease in the travel speed. Thus for a given thickness metal and weld tool, the hot working conditions experienced by the material are expected to be constant when producing a 'good' FSW. A 'good' weld is defined as one without visible defects or significant decrease in the ultimate tensile strength (>30%).

B) Metal Cutting

One method to isolate the shear band proposed in the FSW/P model is the metal cutting process illustrated in Figure 3. Studies reported in the literature indicate a refined microstructure to be present in the metal chips produced during metal cutting processing [16-19]. Similarities or differences in the resulting microstructures between FSW/P versus metal cutting help to quantify the amount of strain versus an initially high strain rate required for grain refinement. Figure 4

illustrates a possible link between the microstructure in shear bands formed during metal cutting and the microstructure observed in FSW/P.

Since the microstructure of a metal responds differently to imposed strain or strain rate at a given temperature, controlled experiments that duplicate the metal hot working conditions can be compared to the microstructure of a FSW nugget. In all materials joined by FSW/P, the nugget is consistently comprised of extremely refined or recrystallized grains. Recrystallization can occur by two processes: a series of strain and annealing stages or by high deformation rates.

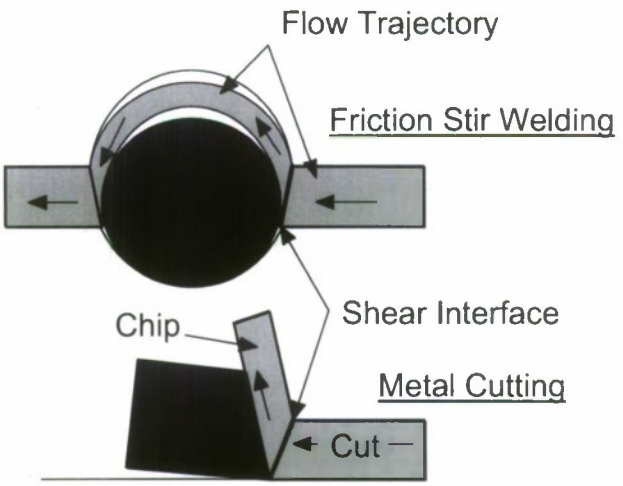

Figure 3. Proposed similarity between friction stir welding and metal cutting processes.

(a) *(b)* *(c)*

Figure 4. Orthogonal metal cutting model proposed as "deck of cards", in which shear bands cause the removed metal to break away (a). Microstructural studies of these shear bands in metal cut chips have shown a heavily deformed microstructure in which grain refinement has been reported (b). Mechanisms responsible for grain refinement within the shear bands maybe similar to that in the FSW/P (c).

If the recrystallization occurs by subjecting the metal to a critical amount of strain with subsequent heating, then the process could be considered using conventional dislocation

processes. The flow path, as influenced by the pin tool features could be designed to ensure the metal is subjected to a critical amount of strain, at the weld temperature to drive the recrystallization process.

However, if the recrystallization occurs by subjecting the metal to a critical strain rate, at a critical temperature, then the process can be considered as grain refinement in the shear zone followed by sustained superplastic flow of metal within the rotating plug. In this case, a critical tool rotation is required to ensure the shear rate is sufficient to drive the recrystallization process. Mechanisms responsible for this grain refinement have been proposed, but not validated [4].

Predictive machining theory has evolved for determining the cutting forces, temperatures, and stresses during metal cutting process [16-18]. Current research into mathematical modeling of the metal cutting process is used to reduce costs and increase quality of machined surfaces. The metal cutting predictive models utilize plasticity theory to analyze the chip formation process [17-19]. This introduces the temperature and strain rate dependant work material flow stress and thermal properties into the analysis. The metal cutting process is considered to be a series of shear fronts that initiate along a line extending from the tool tip to the free surface. The chip formed can be discontinuous, caused by formation of adiabatic shear bands, or continuous, if steady state metal plasticity can be induced.

C) Adiabatic shear band temperature

The temperature increase in the adiabatic shear band can be estimated by equation 3 [5];

$$\Delta T = \frac{\beta \bullet \sigma_{eff} \bullet \varepsilon_{eff}}{\rho \bullet c} \qquad \text{(eqn. 3)}$$

Where β is the fraction of plastic work converted into heat, ρ is the density, and c is the specific heat capacity of materials. The σ_{eff} is the equivalent flow stress and ε_{eff} is the effective strain. They can be calculated by equation 4 and 5 respectively [5]:

$$\sigma_{eff} = \frac{H}{C} \qquad \text{(eqn. 4)}$$

where H is the measured microhardness values and C is the constant (C = 3.0).

$$\varepsilon_{eff} = \frac{\sqrt{3}}{3}\tan(\theta) \qquad \text{(eqn. 5)}$$

where $\theta = 90^{\circ} - \phi$ and ϕ is the shear angle.

Instrumented torsional Gleeble tests were conducted at the Ohio State University. This data will provide information on the effect of varying strain rates on the β transus temperature. This will allow evaluation of the effect on the adiabatic heating as indicates that the β transus is lowered during dynamic tests may result from the increased temperature due to adiabatic shear.

IV. Experimental Procedure

Commereially available Ti-6Al-4V was used during this study. The material was supplied in the annealed condition and rcported by the supplier to eontain 6.1% Al, 4.2% V, 0.08% Fe, 0.01% C, 0.05% N and 0.12% O by weight. Panels used werc 0.635 cm thick.

A) Friction Stir Welding

The as-receivcd PM was cut into panels with dimensions 7.5 x 60 x 6.4 cm. Two pancls wcrc used to create butt joints along the 60 cm lengths of the pancls. The faying surfaees of these butt joints were machined in a horizontal mill prior to joining. Two tapered pin tool designs, 90° and 120° ineluded angle taper, or 45° and 60° half angle taper, were used to FSW the joints. All of the welds were made with a 2.5° lead angle in displacement control. Additionally, all pin tools had a smooth 7° coneave shoulder. All FSWs were made at the NASA-Marshall Space Flight Center with their personnel assisted by MSU graduate students. Table II summarizes the weld schedulcs for the pin tools. Three weld schedulcs wcrc evaluated by varying thc travel rate on cach 60 em long butt joint. Aceeptable FSW schedules wcrc made on the basis of surfaec appearance and radiographic x-ray inspection.

Table II. FSW Process Parameters.

Weld ID	Included Taper angle (°)	Taper angle (°)	Spindle Speed (RPM)	Spindlc Travel (cm/min)
0020W	90	45	400	10.2 - 11.4 - 12.7
0030W	120	60	400	9.5 - 11.4 - 13.3

B) Metal Cutting

Figure 5 shows a schematic of the specimen disk mounted on a lathe with the cutting tool perpendicular to the longitudinal axis of the specimen disc. The specimen disks were machined through the material thiekness of blanks prepared with a recessed diameter to ensurc a free surface at both ends of the cutting tool. This turning operation approximates standard orthogonal cutting conditions [19]. For preliminary studies, chips were formed at two cutting speeds, 1320 and 3420 cm/min (0.22 and 0.57 m/s), at a constant 0.36mm depth of eut and a 5° rake angle. Based on the resulting microstructural analysis, additional metal chips will bc fabricated to expand the range of shear strain rates investigated. A water queneh was applied to the metal chips as they were formed to retain the microstructurc. Tablc III summarizes the cutting conditions and resulting shear strain and shear strain rate.

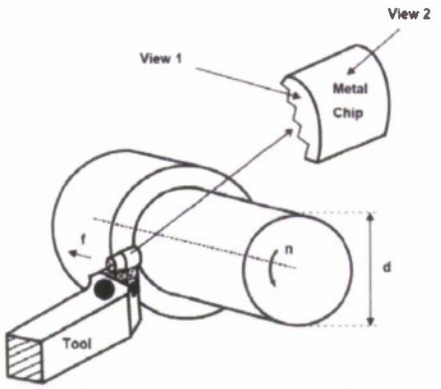

Figure 5. Schematic of metal chip formation during a metal turning operation.

By measuring the cutting speed (V), depth of cut (t), metal chip thickness (t_c), and shear band spacing (Δy), the strain (γ) and strain rate ($\dot{\gamma}$) can be calculated using Equations 6 and 7, respectively [19].

$$\gamma = \frac{\cos\alpha}{\sin\phi \cdot \cos(\phi - \alpha)} \qquad \text{(eqn. 6)}$$

$$\dot{\gamma} = \frac{\cos\alpha}{\cos(\phi - \alpha)} \cdot \frac{V}{\Delta y} \qquad \text{(eqn. 7)}$$

where the shear angle (ϕ), a geometric relationship, is calculated using Equation 8 [19].

$$\tan\phi = \frac{\frac{t}{t_c}\cos\alpha}{1 - \frac{t}{t_c}\sin\alpha} \qquad \text{(eqn. 8)}$$

Table III. Metal cutting process parameters.

Chip ID	Lathe Rotational Speed (RPM)	Lathe Travel (cm/min)	Depth of cut (mm)	Rake angle (°)
70 RPM	70	1320	0.36	5
180 RPM	180	3420	0.36	5

C) Characterization

Representative specimens from all experimental methods were metallurgically mounted and polished to investigate the microstructure. Samples were mounted in conductive phenolic mounts. A Buehler SimpliMet 1000 was used to mount the sections at 150°C with 290 bar pressure for 1:40 minutes. The samples were prepared using standard metallographic procedures

progressing from initial grinding with silica paper to final polishing with 0.05 micron alumina powder. These samples were then etched using a solution of 2mL HF and 100 H_2O for 12 s according to ASTM E407-07 for Ti alloys [20].

Optical micrographs (OM) were recorded using a LEICA DMI 5000 metallographic light microscope and then used to determine average prior β grain size in different locations in the PM and FSW nugget region using ASTM standard E112-96 [21].

Scanning electron microscopy (SEM) images of all specimens were obtained using a JOEL 6500F field emission (FE)-SEM operating at 5kV. An energy dispersive spectrometer (EDS), mounted on the FE-SEM, was used for elemental analysis.

PM and metal chip samples were further characterized using transmission electron microscopy (TEM). Thin foils were made through the 50-80 micron thickness of the metal chips. TEM specimen disks (3mm) were punched from the thinned foil, dimpled on both sides (i.e. cut and free surface), and ion milled to electron transparency. The TEM specimens were examined in a JEOL JEM-100CX TEM operated at an accelerating voltage of 100 kV to obtain bright field image (BFI) and selected area electron diffraction (SAD) patterns.

X-ray diffraction (XRD) data was collected using a Rigaku SmartLab with a step size of 0.01° and a 0.5 s dwell. Specimens from the PM, FSW nuggets, and metal cutting were analyzed. X-ray scans were made normal to the transverse sections of the stir zone and normal to the cut surface of the metal chips. The data was compared to ICDD powder XRD data for pure α and pure β Ti at room temperature [22, 23].

Higher resolution TEM images were obtained under a Oak Ridge National Laboratory (ORNL) SHaRE proposal [24] which provided access to a Hitachi HF-3300 FEG/TEM/STEM. Specimens were prepared using a Hitachi NB-5000 Dual-Beam Focused Ion Beam (FIB) system also at ORNL. Use of the FIB allowed selected regions of the metal chips to be investigated in detail as illustrated in Figure 6. The FIB specimens were 10 high x 20 wide microns and did not encompass the through material thickness of 50-80 microns. Specimens F1 and F2 were removed from the cutting surface oriented along the cutting direction and 90° to the cutting direction. F3 was removed from the free surface.

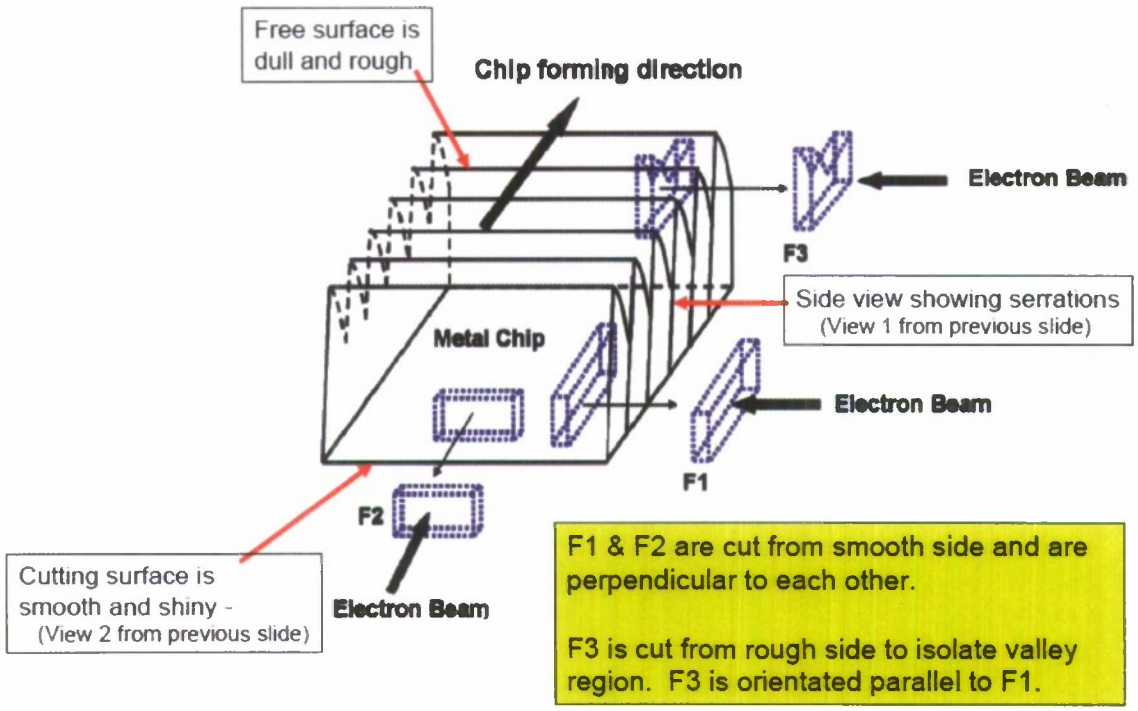

Figure 6. Location of TEM foils removed using FIB.

V. Results

A combination of SEM, TEM, and XRD techniques were used to characterize the as-received PM and experimental specimens. Detailed discussion of the FSW microstructure is documented in [25] and of the metal chips in [26].

A) Parent Material

The starting parent material (PM) was characterized prior to evaluation of the grain refinement degree following FSW/P and metal cutting. The starting microstructure is shown in Figure 7a and contains colonies of alternating α+β laminate within prior b grains. The prior β colony size is 138 μm. Within the β colonies, α colonies are separated by β lathe approximately 1.4 mm wide. The grain boundaries are decorated with α phase approximately 5 μm in thickness with some 5 mm equiaxed grains. Based on SEM images, the two phase microstructure contains approximately 10-12% β. The results are consistent with reference data on Ti 6-4. Figure 7b is a TEM bright field image (BFI) of the parent material which shows the relative thickness of the β and α lamellar microstructure.

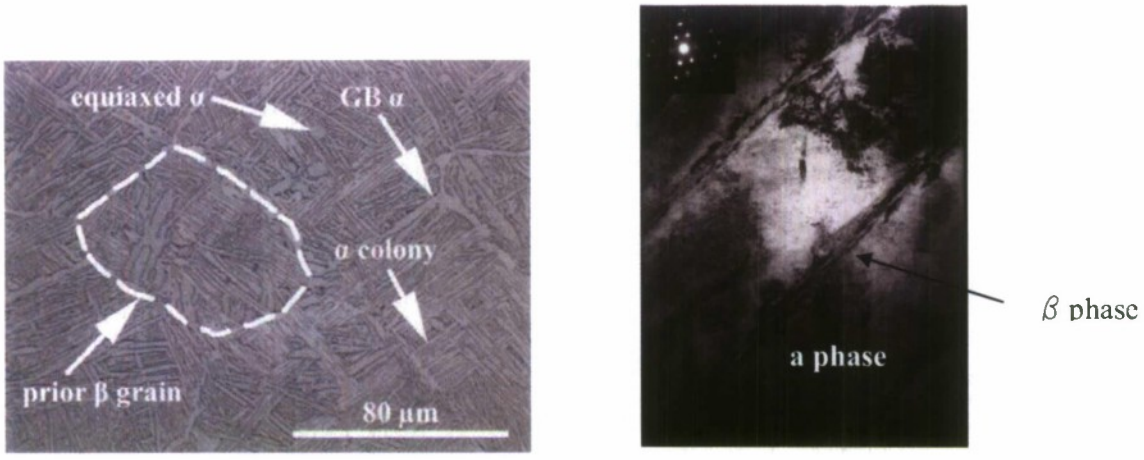

Figure 7. Optical micrograph of the parent material (a) with TEM BFI showing details of lamellar α/β microstructure (b). SAD of the α phase is shown inset in (b).

B) Friction Stir Welds

Using the kinematic model, the shear strain and shear strain rate were estimated for the processing parameters evaluated. The hot working conditions are summarized in Table IV. As mentioned previously, these parameters do not change greatly within the envelope of processing parameters yielding an acceptable FSW.

Table IV. Estimated hot working conditions in FSWs.

Weld ID	Shear strain (in/in)	Shear strain rate (s^{-1})	Estimated Temperature (°. C)
0020W	90-112	2.5×10^3	$950 < T_{FSW} < 1200$
0030W	145-207	4.0×10^3	$950 < T_{FSW} < 1200$

Figure 8a illustrates the typical macrostructure observed in FSW/P with the microstructure of the weld nugget in Figure 8b. The microstructure of the stir zone consisted of grain boundary (GB) α and prior β grains varying in size from about 4-23μm which contained colonies of acicular α. Figure 9 summarizes the grain size in various regions of the weld nugget. This shows a reduction in grain size of approximately 85% from the initial PM of 138 μm. The grain size varied within the nugget region with the smallest grain (~4 μm) located at the bottom of the stir zone as well as smaller grains (~10 μm) located around the top surface of the weld [25].

Qualitative XRD results indicated a change in texture from the as-received material after FSWing as shown in Table V. The XRD data is normalized to the highest intensity (10.1) peak for a randomly oriented powder specimen [22]. The peak intensity ratio show the parent Ti-6Al-4V has a preferred orientation in the (00.2) when compared to International Center for

Diffraction Data (ICDD) results for commercially pure α-Ti [22]. The preferred orientation is most likely due to hot rolling during the manufacturing of the plates. The stir zone, however, contains a more random orientation when compared to the parent material.

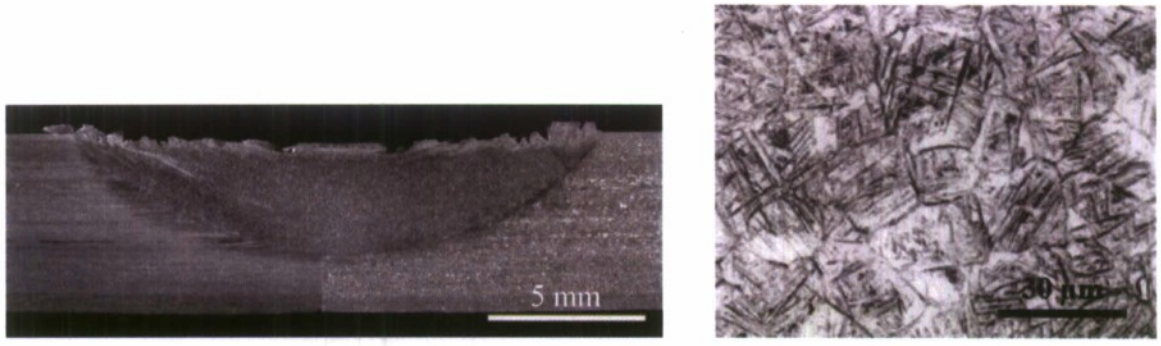

Figure 8. Microstructure of FSW/P nugget in Ti 6/4 (a) with optical microscope image of the nugget grain morphology (b).

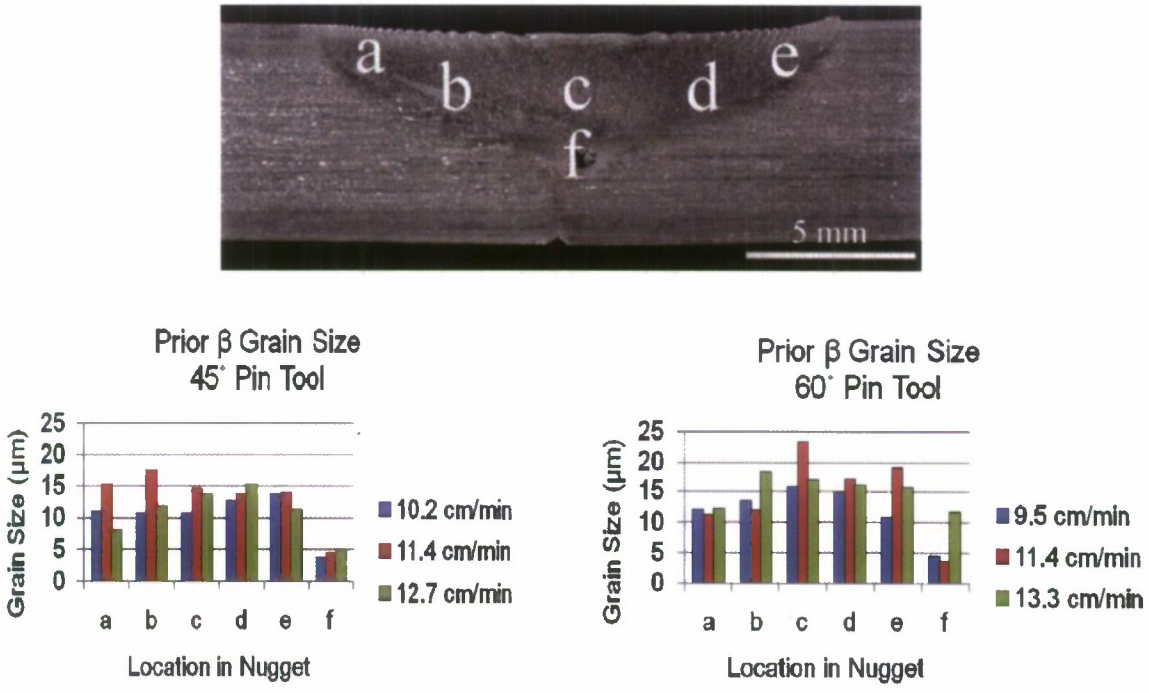

Figure 9. FSW/P refines grains to 85% of starting PM prior β grain size of 138 μm.

The resulting nugget morphology shown in Figure 8b indicated the temperature reached during the FSWing was > 950° C. The FSW tools used remained in tact with no evidence of wear in the FSW nugget. Since the upper temperature limit for structural integrity of the weld tool was 1200° C [27], this also provides an upper bound for the FSW temperature.

Table V. Summary of XRD analysis.

	(10.0)/(10.1)	(00.2)/(10.1)
ICDD α-Ti [22]	0.22	0.24
parent material	0.59	3.12
FSW nugget	0.31	0.73

C) Metal Cutting

To analyze the metal working conditions imposed during the metal cutting operations, the metal chips were mounted and polished for measurement of the as-cut metal chip thickness and spacing between shear planes. Measured chip thickness and the calculated strain, and strain rate are summarized in Table VI. The strain ranged from 4-6 over a strain rate range of 1.1×10^5 to 1.9×10^5 s^{-1}, respectively.

Table VI. Calculated strain and strain rate based on cut metal chip thickness.

Cutting speed (m/s)	Metal chip thickness (μm)	Shear Strain	Shear Strain Rate (s^{-1})	Estimated adiabatic temperature (° C)
0.22	57	6.3	1.1×10^5	414
0.57	81	4.5	1.9×10^5	414

Similar microstructures were found in the metal chips cut at the two conditions, consisting of 6.0 μm equiaxed primary α grains. Typical shear bands, with a width ranging from 1.8 to 2.0 μm, which were present in all chips as shown in Figure 10. In regions of adiabatic shear bands, the β lamellar was observed to thin to 70 nm. The measured volume fraction of β phase in the metal chips ranged from 10 to 12%.

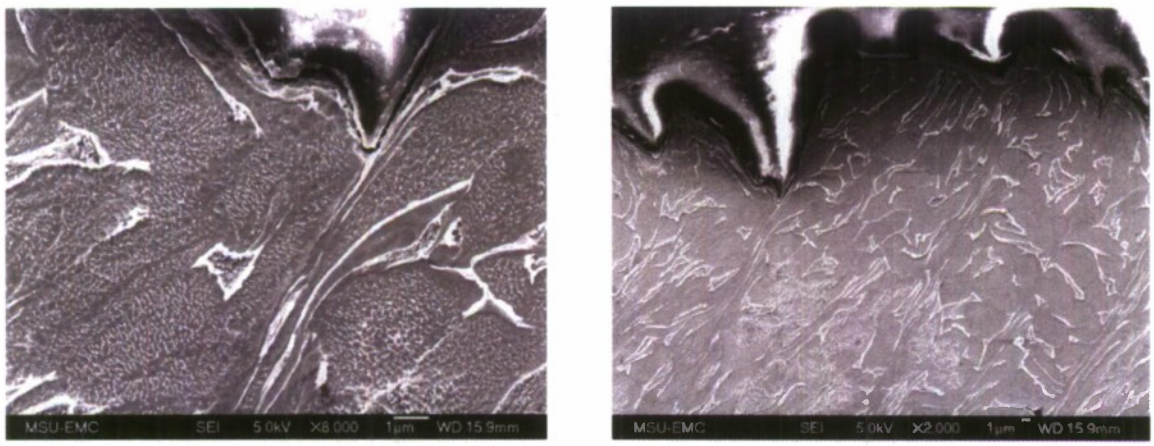

(a) *(b)*

Figure 10. SEM images of the side view of the cut chips (a), a close up of an adiabatic shear band shown in (b).

The XRD peak profiles for the PM and metal are shown in Table VII. As compared with the powder diffraction standard [22], the α-Ti (00.2) peak has the strongest intensity peak corresponding to texture in the rolled plate. The texture observed in the metal chips is similar to that of the PM, although with a corresponding decrease in the (10.0) reflection. A slight peak shift and peak broadening, summarized in Table VIII are evident in the α -Ti phase of the metal chip microstructure which obscures the β-Ti peaks.

Table VII. XRD analysis of the metal chips.

	(10.0)/(10.1)	(00.2)/(10.1)
ICDD α-Ti [22]	0.22	0.24
parent material	0.59	3.12
metal chips	0.22	3.07

Table VIII. Summary of the three primary peak reflections of the α-Ti phase.

hkl	α-Ti [22]	PM		1.1×10^5 s^{-1}		1.9×10^5 s^{-1}	
	2θ (°)	2θ (°)	FWHM	2θ (°)	FWHM	2θ (°)	FWHM
(10.0)	35.09	35.70	0.361	35.42	0.535	35.42	0.471
(00.2)	38.45	38.86	0.330	38.58	0.453	38.54	0.423
(10.1)	40.18	40.80	0.379	40.50	0.525	40.44	0.497

TEM BFI and Selected area diffraction (SAD) patterns indicate a progression toward grain refinement as shown by the spot pattern in Figure 11a and ring pattern in Figure 11b. The lamellar structure is still observed after the metal cutting deformation. The spot pattern is associated with large grains (Fig. 11a) which evolve into a ring pattern (Fig. 11b) when sufficient grains are within the area of aperture. To help in defining the microstructure, the metal chips were subjected to a heat treatment at 260° C for 5 minutes.

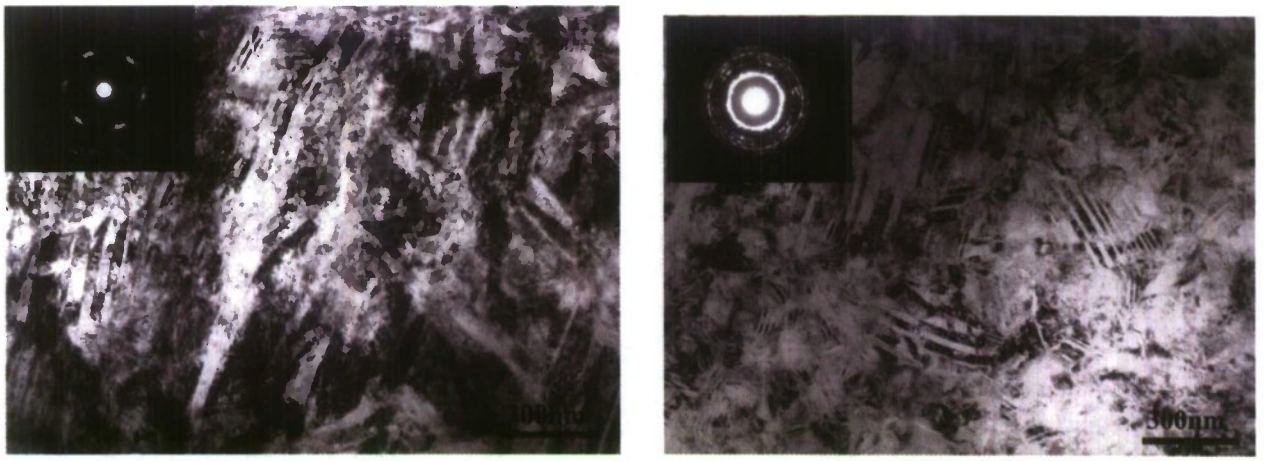

Figure 11. Various regions of the TEM specimen cut from the through metal chip thickness. Some regions show larger grains (a) as compared with smaller grains in other regions (b).

To gain a better understanding of the microstructural features observed in the 100 kV TEM at MSU, The facilities at ORNL were used [24]. TEM specimens were selectively removed using FIB techniques. Specimens close to the cutting surface captured the influence of the severe deformation occurring during metal cutting. Figure 12a and 12b show an overview of the FIB specimens. The height of the specimen is approximately 10 microns, which is roughly 20% of the 80 micron chip thickness. The smooth surface at the top is the cutting surface and the rough edge at the bottom of the image is where it was removed from the chip specimen.

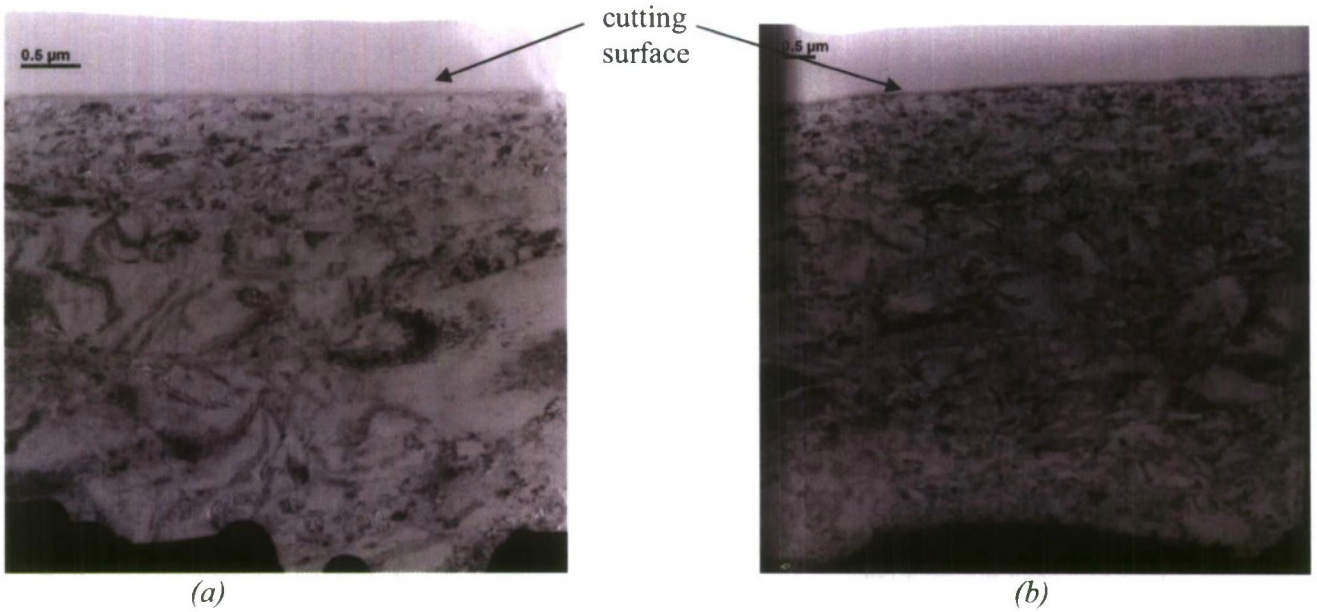

Figure 12. TEM BFI of FIB specimens removed 0 (a) and 90° (b) from the cutting direction.

A close up of the region near the cutting surface is shown in Figure 13 Both equiaxed and elongated grains can be observed in Figure 13b. The elongated grains in this region show banding typical of severe deformation. Figure 14 shows a similar mixture of equiaxed and elongated grains. The regions in Figure 13 and 14 are typical of the microstructure in both the 0 and 90° orientations of the FIB TEM specimens.

To estimate the adiabatic temperature during metal cutting, microhardness measurements were made of the metal chips [28]. The measured hardness of Ti-6Al-4V metal cutting chip with strain rate of 1.9×10^5 s^{-1} was 4.6 GPa. Using a energy conversation constant of $\beta = 0.9$, density of 4.428 kg/m3, and specific heat capacity of 564J/kg*K, the calculated temperature increase inside the adiabatic shear band is 414°C. This is in agreement with the microstructure which indicates the β transus temperature was not exceeded.

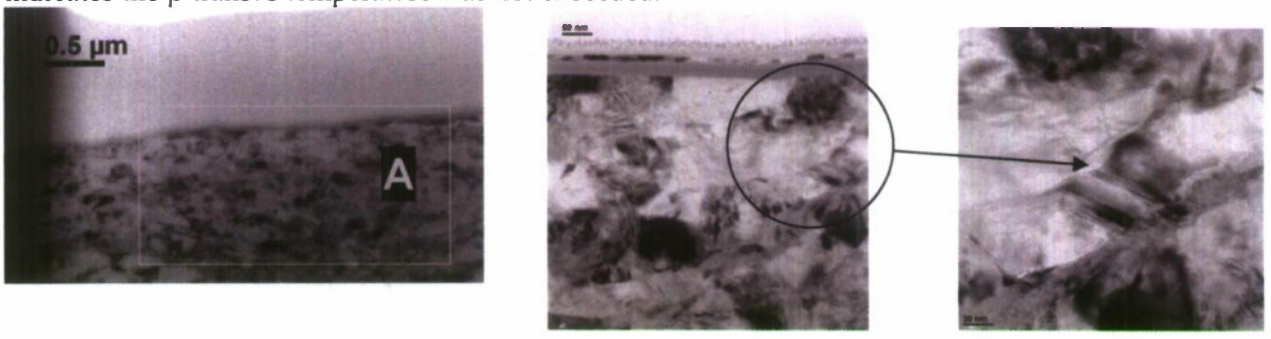

(a) *(b)* *(c)*

Figure 13. TEM BFI showing microstructure close to cutting surface (a). Equiaxed grains are observed along with elongated grains showing evidence of deformation (c).

VI. Discussion

Based on the stir zone microstructure for the FSWs at an estimated shear strain rate of 10^3 s^{-1}, it was apparent that the β transus temperature (950-980°C) was exceeded during all of the welds [2, 3]. The acicular α is contained within prior β grains which were formed while the stir zone was above the β transus [2, 3]. Martensitic microstructure is not present so the cooling rate was not extremely fast (1000°C/min or higher) [2, 3]. The prior β grains in the stir zone are not very large (<30µm) so the cooling rate was not slow enough to keep the material above the β transus long enough to form large β grains [2, 3]. Juhas et al [8], Lienert et al [7], and Zhang et al [29] reported similar findings relating to the cooling rate of Ti-6Al-4V FSWs.

In contrast, after metal cutting at a higher estimated shear strain rate of 10^5 s^{-1}, the initial bi-modal microstructure of the PM was observed to coarsen into equiaxed primary α grains and thickened β plates. Although this reflects elevated temperatures, the β transus temperature of 980°C was not exceeded [2, 3]. These results are in agreement with a numerical modeling study of the metal cutting process in which maximum temperatures of 700°C were predicted [30]. The numerical model used similar cutting conditions to impose a shear strain of ~7 and shear strain rate of $\sim10^5$ s^{-1} [30]. A non-homogenous microstructure was observed in TEM images of the metal chips with evidence of regions of equiaxed and elongated grains.

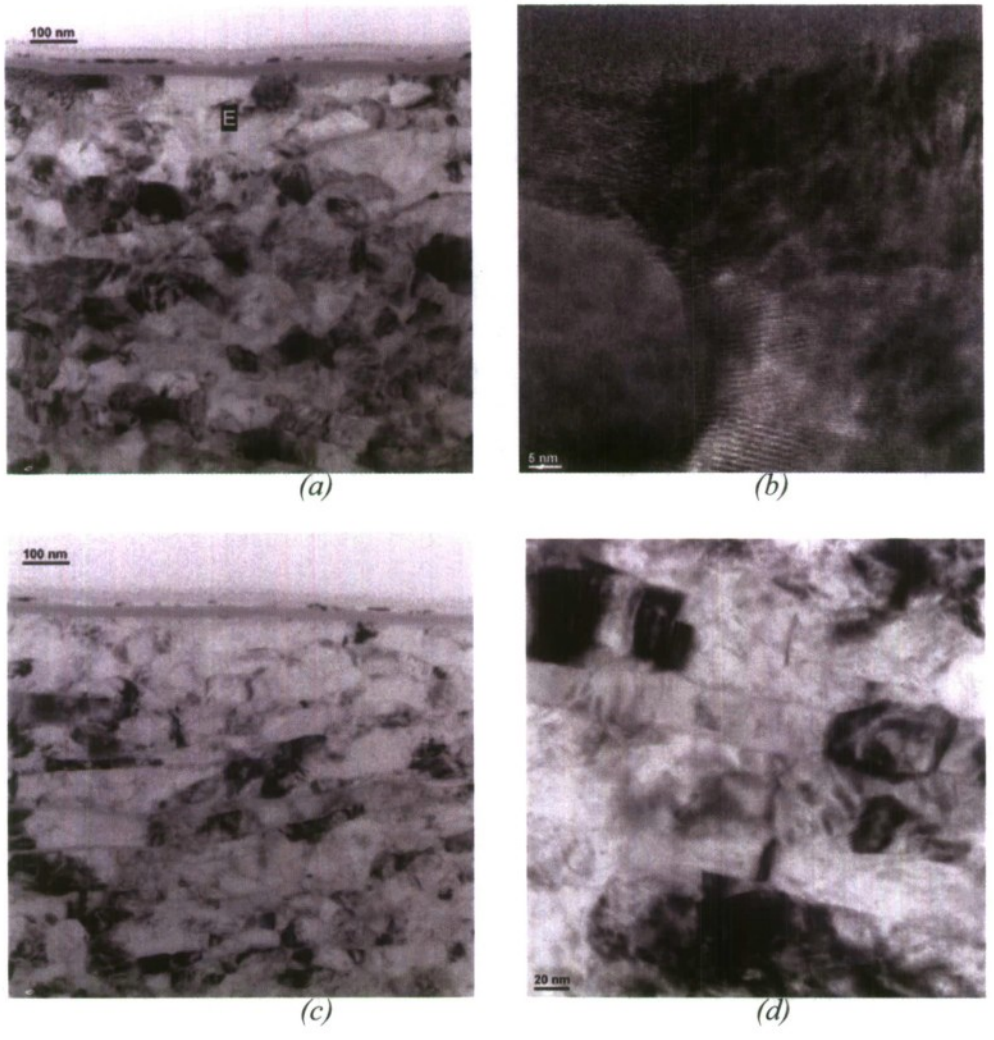

Figure 14. Additional TEM BFI showing evidence of equiaxed and elongated grains (a-c). These microstructural features were observed in both the 0 and 90° specimen orientations with respect to the cutting direction.

Because this microstructure was evident in two orientations with respect to the cutting direction, it can be inferred that the grains were elongated during cutting as evidenced by indicate of severe deformation (Figure 13 and 14). The equiaxed grains may either be regions which may have "pinched off" during deformation or else they may result from cross sectioning of the elongated grains.

The ring patterns observed in the 100 kV TEM studies captured regions of randomly oriented grains. Higher resolution images were able to look at details of the microstructure. SAD patterns could be isolated for the larger grains near the interior of the through metal thickness. However, nearing the cutting surface, the narrow elongated grains gave rise to ring patterns indicating random orientation. No changes were measured in the measured volume fraction of β phase in the PM, FSWs, or metal chips based on SEM images. Although the minor β phase

eould be deteeted in the XRD analysis of the PM, minor peak broadening obseured the β peak in the analysis of the metal ehips and FSW/P speeimens. This indieates the stability of the alloying elements at these elevated temperatures and strain rates.

All eharaeterization teehniques indieate a homogenous FSW nugget forms during FSW/P while a non-homogeneous mierostrueture oeeurs after metal eutting. The FSW/P subjeeted the metal to lower shear strain rates 10^3 s^{-1} at strains >50 and temperatures in exeess of the β transus (>950° C). In eomparison the metal eutting subjeeted the metal to mueh higher shear strain rate of 10^5 s^{-1}, but at eonsiderably lower strains and temperatures. The eonditions imparted by the FSW/P wcre suffieient to reduee the grain size by 85% resulting in equiaxed mierostrueture.

One meehanism of grain refinement at high strain rates has been proposed [4]. However, there has been no experimental verification in the open literature. It has been theorized that torsional deformation ean result in elongation of grains in whieh sub-boundaries form as subjected to elevated temperatures. Torsional deformation eould eventually result in the grains "pinehing off" at the sub-boundaries resulting in refined, equiaxed grains. Subsequent deformation, resulting in grain boundary sliding and rotation, would give rise to randomly oriented grains. This maybe the ease in FSW/P in whieh the rotation tool imparts a torsional deformation to the metal entering the severe shear zone. At the mueh higher levels of strain and temperature, this proposed grain refinement proeess may oeeur. In metal eutting, we may be eapturing the initial stages driving toward grain refinement. Although the shear strain rate was higher, the lower strain and temperature may not have been suffieient to drive eomplete grain refinement. Thus it would be proposed to next obtain ehips at higher shear strain rates and temperatures to study whether the proeess indieates a finer degree of grain refinement. As the grains elongate further, evidenee of sub-boundaries eould be evaluated. This would indieate whether torsional deformation is a neeessary eondition for equiaxed grain refinement.

VII. Summary

Based on the results of the FSW experiment, both weld tools ereated similar mierostruetures within the stir zone at estimated shear strain rates of ~$10^3 s^{-1}$. Based on the strueture within the stir zone, the β transus was exeeeded during FSWing of the Ti with all of the weld tool geometries and proeessing parameters. The heat input is assumed to be due to both frietional heating at the tool shoulder surfaee and adiabatie heating within the shear zone surrounding the weld tool.

In eontrast, the metal ehips eut at the higher shear strain rate of ~$10^5 s^{-1}$ whieh also experieneed similar modes of heating but with faster post eutting queneh, show a resulting mierostrueture with regions of refined and elongated grains. The elongated grains show evidenee of deformation with the overall mierostrueture eonsistent with temperatures below the β transus. This experimental evidenee supports numerieal studies [30] whieh prediet loealized temperatures on the order of 700 °C in the metal eutting proeess.

Torsional Gleeble tests, using the temperature profile from FSWing of Ti samples, will allow independent assessment of the effeet of adiabatie heating at shear strains of up to 100%. This

testing has been completed and the data analysis currently underway. The Gleeble specimens were instrumented to obtain temperature data to evaluate variations in the α to β transformation.

VIII. Follow on studies proposed

Variations in microstructure were observed between metal chips formed during metal cutting and the refined microstructure in a FSW. This variation is attributed to differences in the level of shear strain and the temperature profile. Although the amount of localized heat can be quite high in high strain rate applications, it is also dissipated more rapidly than in FSWing. This localized heat strongly affects the accommodation of strain at the applied strain rate. Additionally, the energy input may cause instabilities in the microstructure, i.e. changing grain shape and size in addition to phase composition.

Specific tasks include:

1) Quantify heat input during metal cutting – separate frictional from deformational heating.
2) Compare microstructures from torsional Gleeble tests at varying shear strains to those obtained in FSWing and metal cutting and evaluate variations in the β transus temperature. .
3) Explore relationships and limits between the balances, at a given temperature, for a given microstructure to accommodate strains at the higher strain rates.
4) Quantify conditions where the strain energy input drives microstructural changes.
5) Initiate collaboration with continuum modeling/material modeling teams.

IX Conclusions

This study will assist in advancing analytical and mathematical modeling of the impact resistance of high strength, high temperature resistant, structural materials by providing physics based, material models. Material models provide the stress versus strain response at different temperatures and strain rates to enable the accurate prediction of the mechanical response to an imposed load or impact condition. How a material responds or accommodates various levels of strain at varying strain rates is controlled by microstructural dependant mechanisms. Within a given range, the stress versus strain response follows various scaling laws. If the imposed strain rate or temperatures cause microstructural changes, then the applicable scaling law for stress versus strain relationships must also change. In addition to the scaling laws, current material models do not capture the following microstructural changes which affect the strain hardening or softening response:

- Texture evolution
- Precipitation kinetics
- Dynamic recovery/recrystallization
- Non-diffusional phase transformations

If the conditions where the changes to the microstructure can be determined in advance of time consuming and costly testing, the amount of mechanical testing, which provides input to the

material models, can be reduced. Material models guided by the evolution of the microstructural would improve and provide a physics based approach for analytical and mathematical modeling of impact conditions. The goal of this study is the development of an experimental method to determine regions where the accommodation of the strain at a given strain rate and temperature changes mechanisms due to microstructural changes. This data would be of interest to developers of material models for development of physics based solutions.

X Results from study to date:

Students completing their studies and participating in research at MSU:

1) Haley Rubisoff completed her MS degree in ME, Summer 2009.
Thesis title: "Microstructural Characterization of Friction Stir Welded TI-6AL-4V."

2) Lei Dong is working toward his PhD degree in ME, scheduled for 2010.
Dissertation title" Modeling the FSW Process using Metal Cutting Theory."

3) Two undergraduates have been employed to assist with this study:
Darryl Murray, BSME Spring 2009
Jason Camp, BSME Fall 2009

Research results have been presented at:

1) Rubisoff, H.A. Schneider, J.A., Nunes, A.C., Jr., "Control of structure in conventional friction stir welds through a kinematic theory of metal flow," FSW&P V, 2009 TMS Annual Meeting, Pittsburg, PA.

2) Rubisoff, H.A., Querin, J.A., Schneider, J.A., "Investigating the effects of pin tool design on friction stir welded Ti-6Al-4V," 2009 TMS Annual Mtg, San Francisco, CA [25].

3) Dong, L., Schneider, J.A., "Microstructural evolution of Ti-6Al-4V during high strain rate conditions of metal cutting," 2009 TMS Annual Mtg, San Francisco, CA [26].

4) Querin, J.A., Rubisoff, H.A., Schneider, J.A., "Effect of weld tool geometry on friction stir welded Ti-6Al-4V," 8th International Conference on Trends in Welding Research Proceedings, Pine Mt., GA, 2008.

In addition, manuscripts are in preparation for:

1) Dong, L, Schneider, J.A., "Microstructural evolution in metal cutting chips of Ti-6Al-4V," in process, MSEA, Summer 2009.

XI Acknowledgements

In addition to the kind support of the AFOSR under the direetion of Dr. Joan Fuller, additional support has been obtained in part by:

X-ray Diffraetometers were purehased under NSF-MRI Grant # DMR-0619773 and the FE-SEM was purehased under NSF-IMR Grant #DMR.0216703 and 02070615.

All FSWs were pcrformed at the NASA- Marshall Spaee Flight Center in eonjunetion with the welding group.

High resolution TEM images were supportcd in part by ORNL's SHaRE User Facility, which is sponsored by the Scientific User Facilitics Division, Office of Basic Energy Seiences, the U.S. Department of Energy. We aeknowledge the guidance of Dr. Jane Howe on the 300 kV TEM and Ms. Dorothy Coffey for the FIB specimen preparation.

Mieroindentation measurements were made at the Hysitron Demonstration Laboratory under the kind support of Mr. Riehard Nay and Mr. Jeremiah Vieregge.

Torsional Gleeble speeimens were tested under the kind support of Dr. John Lippold at the Ohio State University.

XII References

[1] J.A. Sehneider, A.C. Nunes, Jr, "Charaeterization of plastie flow and resulting miero textures in a frietion stir weld," *Met. Trans. B*, Vol. 35, pp. 777-783, 2004.
[2] G. Lutjering, and J.C.Williams, *Titanium*, 2nd edition, Springer, 2007.
[3] M. Donaehie, Jr. *Titanium: A technical guide.* Metals Parks, OH: ASM International. 1988.
[4] R.D. Doherty, D.A. Hughes, et al., "Currcnt Issucs in Rccrystallization: A Review," MSEA, Vol. A238, pp. 219-274, 1997.
[5] M. Elmadagli, A.T. Alpas, "Metallographic analysis of the deformation microstrueture of eopper subjected to orthogonal cutting," *Mat'l Sci. & Engr. A*, Vol. A355, pp. 249-259, 2003.
[6] R.S. Mishra and Z.Y. Ma, "Frietion stir welding and proeessing," *Mater. Sci. Engr. R*, Vol. 50, pp. 1-78, 2005.
[7] T.J.Lienert, et al., "Frietion Stir Welding of Ti-6Al-4V," *Proc. of Joining of Advanced and Specialty Materials*, ASM International, St. Louis, MO, October 2000.
[8] Juhas, M.C. et al., "Mierostruetural Evolution in Ti Alloy Frietion Stir Welds," Proc. of *2nd International Symposium on Friction Stir Welding*, Gothenberg, Sweden, June 2000.
[9] J.A. Sehneider, "Use of Marker studies to study material flow in thc frietion stir weld proeess," NASA-CR-2004/213285, p. XXXVIII-1 to -5, August 2004.
[10] J.A. Schneider, A.C. Nunes, Jr., "Thermo-Meehanieal Proeessing in Frietion Stir Welds", Frietion Stir Welding and Proeessing II, ed. K.V. Jata, M.W. Mahoney, R.S. Mishra, S.L. Semiatin, T. Lienert, pub. TMS, March 2003, p. 43-51.
[11] J.A. Sehneider, R. Beshears, A.C. Nunes, Jr., Interfaeial stieking and slipping in the frietion stir welding process", *Mat'l Sci. & Engr. A*, Vol. 435-436, pp. 297-304, 2006.

[12] J.A. Schneider, A.C. Nunes, Jr., "Unraveling the microstructural flow path variations in friction stir welding, Friction Stir Welding and Processing III, ed. K.V. Jata, M.W. Mahoney, R.S. Mishra, S.L. Semiatin, T. Lienert, pub. TMS, Febr. 2005, San Francisco, CA.
[13] J.A. Schneider, A.C. Nunes, Jr., "Quantifying the microstructural flow path parameters in friction stir welding, 7th Int'l Conf. on Trends in Welding, May 2005, Pine Mt., GA.
[14] J.A. Schneider, A.C. Nunes, Jr., "Unraveling the processing parameters in friction stir welding," AeroMat 2005.
[15] Sanders, J.R., Schneider, J.A., Nunes, Jr., A.C., "Tracing material flow paths in friction stir welds," Conference Proceedings, MS&T, Sept. 26-28, 2005, Pittsburg, PA.
[16] M.E. Merchant, "Mechanics of the metal cutting process II. Plasticity conditions in orthogonal cutting," *J. Appl. Phys.*, Vol. 16, p. 318-324, 1945.
[17] P.L.B. Oxley, The Mechanics of Machining, Ellis Horwood Limited, 1989.
[18] J.T. Black, J.M Huang, "Shear Strain Model in Metal Cutting," MED-Vol. 2-1/MH-Vol. 31. Manfgt. Sci. & Engr., *ASME* 1995.
[19] M.C. Shaw, Metal Cutting Principles, Oxford University Press, Clarendon, 1984.
[20] ASTM Standard E407-07, "Standard Practice for Microetching Metals and Alloys," ASTM International, West Conshohocken, PA, www.astm.org.
[21] ASTM Standard E112-96, "Standard Test Methods for Determining Grain size," ASTM International, West Conshohocken, PA, www.astm.org.
[22] International Center for Diffraction Data, PDF #44-1294, Titanium- α, www.icdd.com.
[23] International Center for Diffraction Data, PDF #44-1288, Titanium- β, www.icdd.com.
[24] SHaRE Project ID: 09_SchneiderJ_01, "Transmission Electron Microscopy (TEM) Study of Shear Bands in Metal Chips of Ti-6Al-4V", POC: Jane Howe, POP: March 3, 2009 to March 04, 2011.
[25] H. Rubisoff, J. Querin, D. Magee, J. Schneider, "Microstructural Evolution in Friction Stir Welding of Ti-6Al-4V," Conference Proceedings, MS&T 2008, Pittsburg, PA.
[26] L. Dong, J.A. Schneider, "Microstructure evolution in cut metal chips of Ti-6Al-4V," Conference Proceedings, MS&T, Pittsburg, PA, 2008.
[27]. M. Dennis, Dennis Tool Company, Personnel Conversation, Spring 2008.
[28] Hysitron Demonstration Laboratory, Summer 2009.
[30] Zhang, Y. et al., "Microstructural characteristics and mechanical properties of Ti-4Al-6V friction stir welds," *Mater. Sci. Eng. A,* Vol. A485, pp. 448-455, 2008.
[31] M. Calamaz, D. Coupard and F. Girot, A new material model for 2D numerical simulation of serrated chip formation when machining titanium alloy Ti-6Al-4V, *Int. J. Mach. Tool. & Manuf.*, Vol. 48, pp 275-288, 2008.